Novel x-ray attenuation mechanism: Role of interatomic distance

Steven Poelzing,[a] Adam F. Smoot, and Rengasayee Veeraraghavan
Nora Eccles Harrison Cardiovascular Research and Training Institute and Bioengineering, University of Utah, 95 South 2000 East, Salt Lake City, Utah 84112

(Received 11 December 2007; revised 29 July 2008; accepted for publication 30 July 2008; published 11 September 2008)

Little progress has been made over the last 30 years for improving attenuation by x-ray contrast agents, in part because the mechanisms of x-ray attenuation are thought to be well understood. We hypothesized that x-ray absorbance can be modulated by altering the interatomic spacing between K-edge attenuating atoms. Iodomethane, diiodomethane, 2,6-diiodo-4-nitroanaline, and diiodobenzene isomers were dissolved in DMSO and imaged with an OEC Compact 7600 fluoroscope. At a tube voltage of 42 kVp, absorbance of equimolar diiodomethane (150 mM) was significantly ($p<0.01$) greater than iodomethane (150 mM) by 45%. Interestingly, 150 mM diiodomethane absorbance was significantly greater than 300 mM iodomethane (by 5%, $p<0.01$) despite equal amounts of iodine in both solutions. 1,3-diiodobenzene absorbance was significantly greater than 1,2- and 1,4-diiodobenzene ($p<0.01$). However, 2,6-diiodo-4-nitroanaline absorbance was similar to 1,3-diiodobenzene. When a linear model was fit for absorbance as a function of density and harmonic error (the fractional remainder of the inter-iodine distance and the K-shell ionizing wavelength) at different beam energies, a significant overall fit was obtained for both unfiltered and hardened beams ($p<0.01$). While the slope of absorbance as a function of harmonic error was significant for all conditions ($p<0.01$), the slope with respect to density was significant only when the beam was unfiltered ($p<0.05$). Also harmonic error, but not density, displayed significant energy-dependent effects on absorbance ($p<0.01$). These data suggest that harmonic error is a strong determinant of absorbance, particularly when the beam energy is concentrated near the iodine K-edge and is likely a descriptor of K-characteristic photon interactions. Therefore, x-ray absorbance may be modulated by the distance between covalently linked x-ray K-edge attenuating atoms. This finding has important implications for increasing contrast agent absorbance as well as for designing molecular transducers capable of modulating K-edge attenuating atomic distances and thereby x-ray absorbance. © *2008 American Association of Physicists in Medicine*. [DOI: 10.1118/1.2975151]

Key words: x-ray, K-shell, absorbance, iodine

I. INTRODUCTION

Within two years of Roentgen's demonstration of x-ray based imaging, Walter B. Cannon demonstrated that a bismuth subnitrate capsule could be used to visualize the mechanism of swallowing in a goose.[1] This represents one of the first uses of an x-ray contrast enhancing agent in a biological system. Since then, contrast enhancing media, or "contrast agents," have evolved over the past century to the current state of well tolerated and highly efficacious molecules used in the vast majority of clinical x-ray examinations. Research during the past half century has focused mainly on the development of agents with limited biotoxicity[2–4] and in some respects on agents that can provide enhancement of specific anatomical markers such as blood vessels[5] and plaques.[6]

X-ray absorbance offers a unique imaging modality in that matter is highly permeable to x rays until the energy of the incident x-ray photon corresponds to the energy level of the innermost orbital of an atom (K-shell).[7] At this K-edge, absorbance significantly increases and then again falls as the incident x-ray energy increases further. We hypothesized that x-ray absorbance can be modulated by altering the interatomic spacing between K-edge attenuating atoms on a molecule.

In this article, we demonstrate that absorbance of a polychromatic x-ray beam can be modulated by the distance between covalently linked strong x-ray attenuating atoms such as iodine. Specifically, x-ray absorbance is lowest when the interatomic distance of iodine atoms is closest to a harmonic of the wavelength required for photoelectric interaction with the innermost electron orbital (K-shell). X-ray absorbance increases as the fractional distance between iodine atoms, relative to the photon wavelength necessary for K-shell attenuation, increases.

II. METHODS

II.A. Phantom

The phantom consisted of two aluminum plates with four wells of 2 cm diameter and 1 cm depth compressing a glass microscope slide (Corning Glass Works, Corning, New York), as seen in Fig. 1. Leak between the top compressing aluminum plate and the cover slip was prevented by the in-

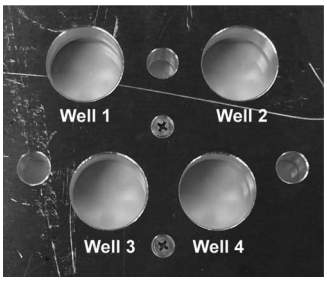

FIG. 1. The aluminum phantom has four wells capable of holding 2 ml samples of solution. The three smaller empty wells were used as controls between recordings.

clusion of a neoprene O-ring. Each well was filled with 2 ml of solution for imaging such that the x-ray path length through each sample was constant.

II.B. Solutions

The following substances were dissolved in 10 ml of dimethyl sulfoxide (DMSO) and then aliquotted into 2 ml of solution per well: Iodomethane (100, 150, 200, and 300 mM), iododecane (100 mM), nonane (100 mM), diiodomethane (150 mM), 1,2-diiodobenzene (150 mM), 1,3-diiodobenzene (150 mM), 1,4-diiodobenzene (150 mM), and 2,6-diiodo-4-nitroaniline (150 mM). All compounds were >98% pure and obtained from Sigma-Aldrich.

II.C. Absorbance

Absorbance was measured with an OEC Compact 7600 fluoroscope. For the non-energy-dependent measurements, the peak applied tube voltage (tube voltage) was 42 kVp (±5% according to manufacturer). The half-value layer (HVL) for peak tube voltages (kVp) were measured using a Triad TNT 35050AT dosimeter with a 15 cm^3 ion chamber (model 96035B), last calibrated within 2 months of all experiments. The filter set was the Fluke HVL filter set (model 37668) of aluminum coupons. The total attenuation coefficient for each effective energy was determined using the XCOM calculator from NIST. Beam quality parameters are listed in Table I. Current was 0.5 mA (±5% according to manufacturer), and all samples were exposed for 0.5 s. The fluoroscope was in full manual mode. Tube voltage was varied to determine the relationship between absorbance and x-ray energy. The output of the fluoroscope was connected via BNC to a National Instruments data acquisition card. Fifty frames were acquired and temporally averaged using custom software written in MATLAB (Mathworks, Natick, Massachusetts) to quantify absorbance per well. Absorbance (A) for each liquid sample was estimated by the Beer-Lambert equation:

$$A_n = -\log_{10}\left(\frac{I_{S,n}}{I_{E,n}}\right). \quad (1)$$

The value n indicates the well number as shown in Fig. 1. I_S corresponds to the grayscale image intensity of the sample. I_E corresponds to the grayscale intensity of the empty well which we equate with the intensity of the incident light that reaches the detector. Therefore, $I_{S,n}/I_{E,n}$ is the transmission factor.

The theoretical transmission factor was calculated with:

$$\frac{I}{I_o} = e^{-(\mu/\rho)x\rho}. \quad (2)$$

μ/ρ is the mass attenuation coefficient obtained from the XCOM database and x is the path length through a sample (1.2 cm).

TABLE I. Beam quality.

kV	HVL (mm Al)	Effective energy
40	2.5	33.4
42	2.6	33.5
44	2.8	34.5
46	2.9	35.3

II.D. Density

One milliliter of each solution was weighed in a Mettler Toledo AL54 precision balance in order to determine the density in g/ml (n=16 for each compound). Theoretical density for liquid compounds was estimated by the following equation:

$$d_S = \frac{[V_u{}^*\rho_u + (1000 - V_u)^*\rho_v]}{1000}. \quad (3)$$

V_u=Solute volume added per ml of solution in microliters. ρ_u=Solute density. ρ_v=Solvent density.

II.E. Molecular dynamics

Chemsketch (Advanced Chemistry Development, Inc. Toronto, Ontario) was used to generate energetically optimized three-dimensional structures for all molecules. Molecular mechanics with force fields are based on CHARMM parametrization.[8] Interiodine distance (d_I) was quantified from iodine nucleus to nucleus. The harmonic error (E_H) is quantified as the fractional remainder of the interatom distance (d) and the wavelength of the photon necessary for K-shell photoelectric attenuation (λ_K):

$$E_H = \frac{d_{\mathrm{I,I}}}{\lambda_{\mathrm{K,I}}} - \left\lfloor \frac{d_{\mathrm{I,I}}}{\lambda_{\mathrm{K,I}}} \right\rfloor \quad (4)$$

For two iodine atoms on a molecule, the inter-atomic distance is $d_{\mathrm{I,I}}$ and the wavelength for K-shell photoelectric attenuation ($\lambda_{\mathrm{K,I}}$) is 0.375 Å. $\lfloor\ \rfloor$ is the floor function. E_H is bounded by the interval [0,1].

II.F. Statistics

The four wells per phantom were averaged to yield the average absorbance for a particular experiment. Each experiment was repeated (n=6, unless otherwise noted). Significance between two measurements was quantified by un-

paired, two-tailed Student's *t*-tests assuming equal variance. A $p<0.05$ was considered statistically significant. All composite measurements are presented as mean ±S.E.M.

A linear model for absorbance as a function of density and harmonic error (E_H) with beam energy as a factor was fit using the statistical package R (The R Foundation, Vienna Austria).

III. RESULTS

III.A. Validation

Since the fluoroscope emits a polychromatic conical beam, it was important to determine interwell transmission variability. Raw uncorrected images of the phantom in Fig. 2(a) demonstrate relative x-ray transmitted intensity (I_B) heterogeneity within and between empty wells at 42 kVp tube voltage. X-ray intensity was greatest in well 1, as evidenced by the greater number of lighter pixels relative to all other wells. The maximal difference between wells was on the order of 30 arbitrary absorbance units, as illustrated by the color bar range in Fig. 2(a). The edges of each well appeared to have lower intensity values than the center of the well, which may have been due to the concave meniscus of the solution. Therefore, to minimize edge effects, the black circle in each well of Fig. 2(a) indicates the region of interest (ROI) from which absorbance was measured. ROI area was constant for all wells, and total x-ray absorbance was quantified as the average absorbance within the ROI. The average intensity for empty wells 2, 3, and 4 ($n=46$) were significantly different relative to well 1 (*, $p<0.01$). However, when absorbance for 100 mM iodomethane was quantified [Eq. (1)], there were no significant differences between wells [Fig. 2(b), gray bars, no significance relative to well 1].

Likewise, increasing concentrations of iodomethane increased absorbance in a linear fashion for all wells as demonstrated in Fig. 2(c) ($n=5$, per concentration). The four wells were separated from each other on the *x*-axis for the purpose of visualization, and this had no effect on the calculated slope. For each well, the correlation coefficient was greater than 0.9 and slopes were not significantly different [Fig. 2(c), table insert].

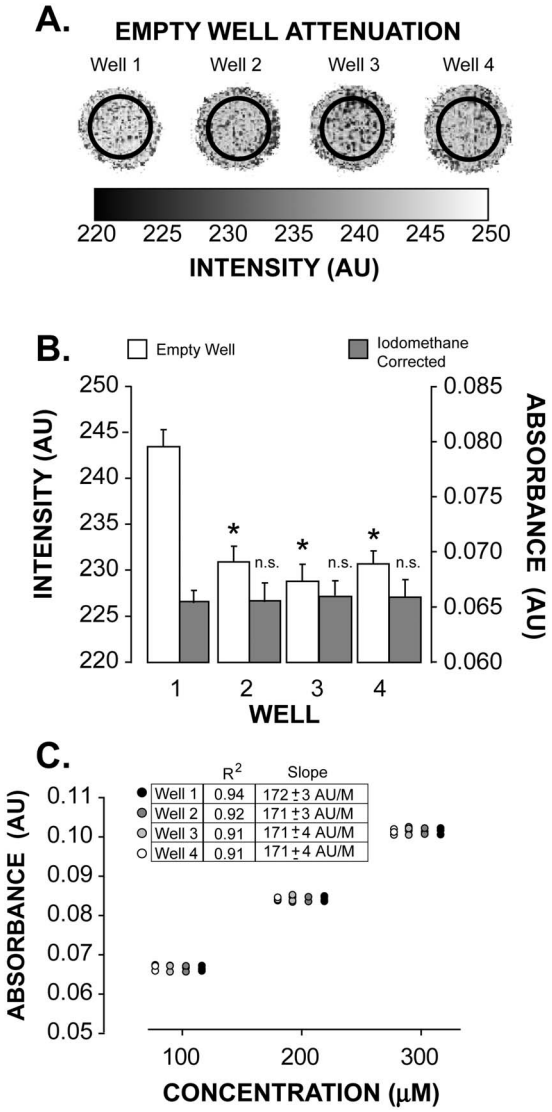

FIG. 2. Calibration of wells removes interwell variability. (A) Representative x-ray images from the four wells demonstrates unequal absorbance properties per well. (B) Summary data demonstrate that empty wells 2, 3, and 4 (white bars) have significantly higher absorbance values than well 1 (*, $p<0.01$). After calculating absorbance using Beer-Lambert's law, there were no significant (n.s.) absorbance differences of iodomethane between wells (gray bars). (C) Absorbance for each well increased linearly as the concentration of iodomethane was increased. The inset provides the linear fit parameters, demonstrating that there was no significant difference between wells.

III.B. Iodo-alkanes

Equimolar (150 mM) iodomethane (CH_3I) absorbance (42 kVp tube voltage) without and with nonane (C_9H_{20}, 150 mM) was compared to 100 mM iododecane ($C_{10}H_{21}I$) absorbance in Fig. 3. Iodomethane+nonane together have an equal number of iodine and carbon atoms relative to iododecane, but iododecane has two fewer hydrogen atoms. Representative images of an empty well, iodomethane, iodomethane+nonane ($CH_3I+C_9H_{20}$) and iododecane demonstrates relative x-ray absorption between samples (Fig. 3(a)). The empty well is provided for contrast. The image intensity of iodomethane (100 mM) was significantly higher than iodomethane (100 mM)+nonane (100 mM) indicating lower absorbance for iodomethane. Covalently bonding nonane to iodomethane, to make iododecane (100 mM), increased absorbance above iodomethane and iodomethane +nonane. Summary data from all experiments in Fig. 3(b) demonstrate that iodomethane+nonane and iododecane absorbance is significantly greater than absorbance of iodomethane alone by 26% and 31%, respectively. Additionally, iododecane absorbance was significantly more than iodomethane+nonane absorbance by 4%. Both theoretical and experimentally measured iodomethane solution densities were significantly greater than both iodomethane+nonane and iododecane solution densities as demonstrated in Table II.

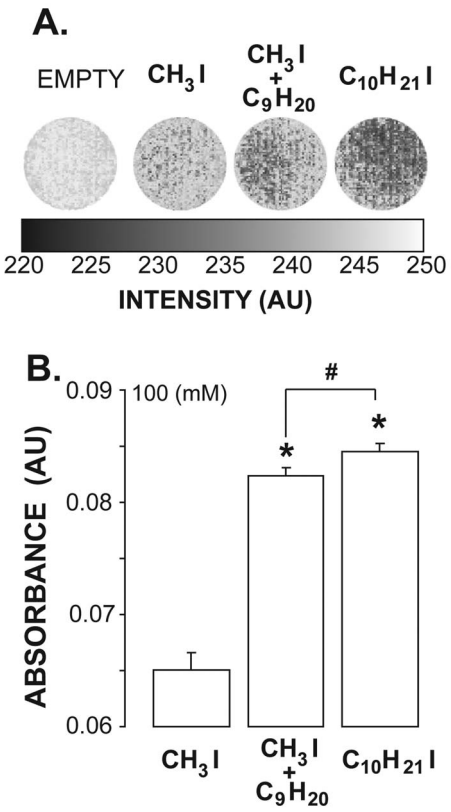

FIG. 3. Density and the mixture rule do not always explain absorbance differences. (A) Representative images of an empty well, iodomethane (CH_3I), iodomethane+nonane ($CH_3I+C_9H_{20}$), and iododecane ($C_{10}H_{21}I$). (B) Summary data demonstrates that iododecane absorbance was significantly greater than iodomethane+nonane absorbance (#). Iododecane and iodomethane+nonane absorbance was significantly greater than absorbance of iodomethane alone (*). However, iodomethane is denser than iodomethane+nonane and iododecane (Table II).

III.C. Iodomethane versus diiodomethane

X-ray images of an empty well (provided for contrast) and wells with 150 mM diiodomethane (CH_2I_2), 150 mM iodomethane (CH_3I), and 300 mM iodomethane are shown in Fig. 4(a) (42 kVp tube voltage). Absorbance due to diiodomethane (CH_2I_2) was greater than absorbance due to equimolar iodomethane as expected. This is summarized in Fig. 4(b) (*, $p<0.01$, $n=16$ for all compounds).

Representative and summary data in Fig. 4 demonstrate that twice the concentration of iodomethane (2× iodomethane, 300 mM) absorbance is significantly lower than diiodomethane (1× diiodomethane, 150 mM) absorbance. The number of iodine atoms was equal in both solutions. For all experiments, 1× Diiodomethane (150 mM) absorbance was significantly greater than 2× iodomethane absorbance [Fig. 4(b)]. The densities of the 1× and 2× iodomethane solutions (estimated and measured in Table II) were less than diiodomethane.

Experiments were repeated with the fluoroscope set to voltages of 40, 42, 44, and 46 kVp with and without the use of a 3 mm thick aluminum plate placed on the beam output to harden the beam. Summary data in Fig. 5 demonstrate that for both unhardened and hardened beams, x-ray absorbance

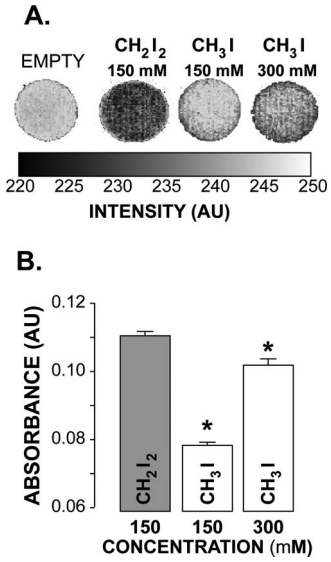

FIG. 4. Diiodomethane absorbance was significantly greater than the absorbance of twice the concentration of iodomethane. (A) Representative images of an empty well, diiodomethane, iodomethane, and twice the concentration of iodomethane (300 mM). (B) Summary data demonstrate that 150 mM iodomethane and 300 mM iodomethane absorbance was significantly less than diiodomethane absorbance (*).

for iodomethane (both concentrations) and diiodomethane compounds significantly decreased with increasing energy. Diiodomethane absorbance was significantly greater (*, $p<0.01$) than iodomethane and 2× iodomethane absorbance for all tube voltages, consistent with results at 42 kVp.

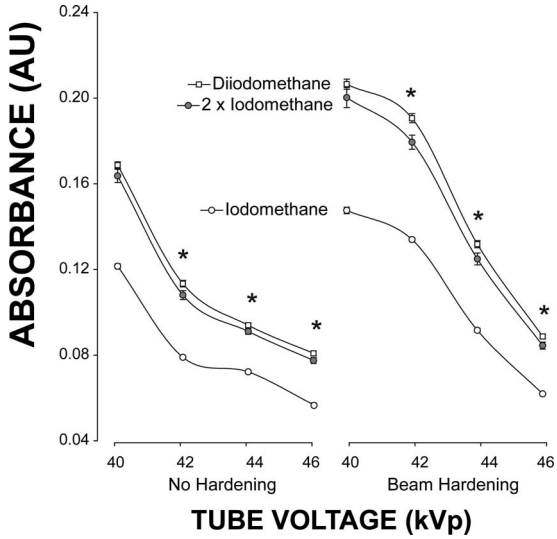

FIG. 5. Increasing x-ray energy decreases absorbance, and beam hardening increases absorbance. Diiodomethane (150 mM) absorbance was significantly greater than the absorbance of equimolar iodomethane (Iodomethane) and twice the concentration of iodomethane (2× Iodomethane) at tube voltages of 42, 44, and 46 (*, $p<0.01$). With beam hardening, the same was true. Additionally, beam hardening significantly increased absorbance by all three samples. The relative absorbance differences between 150 mM diiodomethane, 150 mM iodomethane, and 300 mM iodomethane decreased as tube voltage increased.

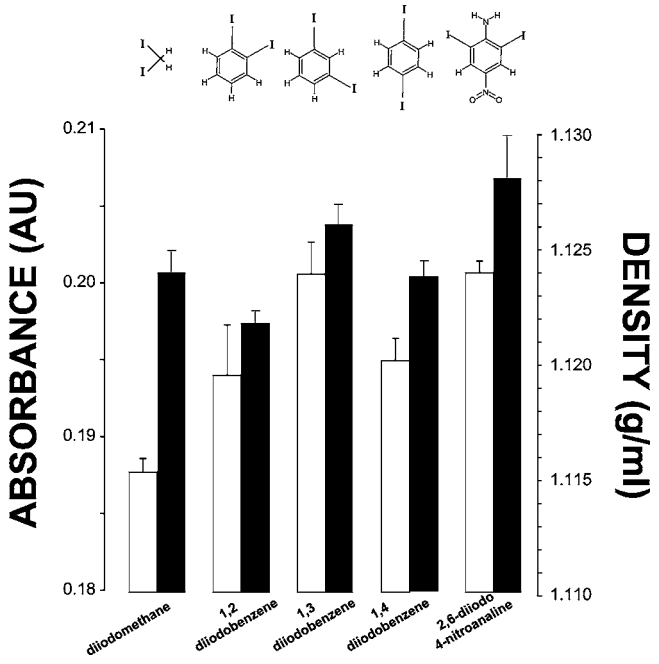

FIG. 6. Absorbance correlates with the harmonic error at low energies and density at high energies. The molecular sketch of each compound is shown above the absorbance (white bars) and measured density (black bars) of each compound. 1,3-diiodobenzene and 2,6 diiodo-4-nitroaniline absorbance was significantly greater ($p<0.01$) than other compounds. Diiodomethane absorbance was significantly less ($p<0.01$) than all other compounds.

Beam hardening increased absorbance for all samples and the separation of absorbance between diiodomethane and 2× iodomethane at 42 and 44 kVp. This difference was attenuated at a tube voltage of 46 kVp. Specifically, the difference between diiodomethane and 2× iodomethane absorbance measured at a tube voltage of 42 kVp was significantly greater than the difference between the two substances at either 44 or 46 kVp tube voltages (0.010 ± 0.002 [42 kVp], 0.005 ± 0.001 [44 kVp], and 0.002 ± 0.001 [46 kVp]).

III.D. Diiodobenzenes

Absorbance was quantified for 2,6-diiodo-4-nitroaniline and three positional isomers of diiodobenzene ($C_6H_4I_2$) (1,2-diiodobenzene, 1,3-diiodobenzene, and 1,4-diiodobenzene). The diiodobenzenes were chosen because, like diiodomethane, the iodine atoms are at fixed distances from each other. Furthermore, the diiodobenzenes have identical chemical formulae removing the confounding influence of electrons per gram of solute. The compound 2,6-diiodo-4-nitroaniline also has iodine atoms at fixed distances from each other and an additional electron withdrawing nitro group that modulates the interiodine distance.

Figure 6 presents absorbance of all compounds with beam hardening at a tube voltage of 42 kVp (white bars). Diiodomethane absorbance was significantly less than all other compounds ($p<0.05$). In specific diiodomethane absorbance was 3%, 7%, 4%, and 7% less than the absorbances of 1,2-diiodobenzene, 1,3-diiodobenzene, 1,4-diiodobenzene, and 2,6-diiodo-4-niotroanaline respectively. On the other hand, 1,3-diiodobenzene and 2,6-diiodo-4-nitroaniline absorbance was significantly greater than all other compounds. Additionally, 2,6-diiodo-4-nitroaniline absorbance was not significantly different from 1,3-diiodobenzene absorbance ($p<0.05$). Collectively, 1,3-diiodobenzene and 2,6-diiodo-4-nitroaniline absorbance was approximately 3% greater than 1,2-diiodobenzene and 1,4-diiodobenzene absorbance.

TABLE II. Solution density for all compounds dissolved in DMSO were estimated when the compound was liquid at room temperature. N/A refers to compounds solid at room temperature where density could not be estimated. Experimental density was measured as described in Sec. II.

	Estimated density (g/ml)	Experimental density (g/ml)
Iodomethane	1.1121	1.1120 ± 0.0021
Iodomethane (300 mM)	1.1158	1.1128 ± 0.0019
Iodomethane+Nonane	1.1013	1.1001 ± 0.0015
Iododecane	1.1059	1.1031 ± 0.0012
Diiodomethane	1.1282	1.1211 ± 0.0011
1,2-Diiodobenzene	1.1295	1.1219 ± 0.0008
1,3-Diiodobenzene	N/A	1.1262 ± 0.0021
1,4-Diiodobenzene	N/A	1.1239 ± 0.0009
2,6-Diiodo-4-Nitroaniline	N/A	1.1281 ± 0.0023

The density for each compound (150 mM, unless otherwise noted) in DMSO is listed in Table V. The experimentally measured density of each compound is graphed in Fig. 6 (black bars) next to absorbance (white bars) for visual comparison. There were no significant empirical differences in density between compounds. However, 2,6-diiodo-4-nitroaniline trended towards a significantly greater density than all other compounds ($p=0.10$).

A linear model for absorbance as a function of density and harmonic error [Eq. (4)] with tube voltage as a factor was fit using R. The equations are provided in Tables III and IV. For the two cases, without and with beam hardening, the results obtained are summarized in Tables III and IV, respectively.

In both cases (without beam hardening, and with beam hardening), the overall fit of the linear model to the data was significant ($p<0.001$). Also, the slope of absorbance as a function of E_H was significant for both cases (k_{E_H}, $p<0.001$) whereas the slope of absorbance as a function of density was significant (k_ρ, $p<0.05$) only when the beam was unhardened. Further, the slopes obtained for the energy-dependent effects of density (k_ρ^E) were not significant, regardless of whether the beam was hardened or not.

There was a decrease in the slope of absorbance as a function of E_H at higher energies ($k_{E_H}^E$), as evidenced by the negative slopes obtained for the energy dependent effect of E_H at energies of 42, 44, and 46 kVp when the beam was unhardened and hardened. However, the absolute value of these negative slopes was smaller than the slope for the energy-independent effect of E_H (k_{E_H}), indicating that a positive correlation between absorbance and E_H exists for all measured tube voltages. Furthermore, the negative slopes for the energy-dependent effects of E_H ($k_{E_H}^E$) were significant

TABLE III. Parameters for a linear model of absorbance (A) as a function of harmonic error (E_H) and density (ρ) at different beam energies (E) without beam hardening. The model includes both energy-dependent and energy-independent relationships of absorbance to E_H and density. Linear model: $A=(I+I^E)+(k_{E_H}+k_{E_H}^E)\times E_H+(k_\rho+k_\rho^E)\times\rho$.

Coefficients	Estimate	Std. Error	p
INTERCEPT (I)	−0.278 480	0.202 474	0.170
as.factor(Energy)42 (I^{42})	0.241 674	0.286 342	0.399
as.factor(Energy)44 (I^{44})	0.192 192	0.286 342	0.503
as.factor(Energy)46 (I^{46})	0.015 225	0.286 342	0.958
SLOPE			
E_H (k_{E_H})	0.019 410	0.002 956	**<0.001**
E_H:as.factor(Energy)42 ($k_{E_H}^{42}$)	−0.008 662	0.004 180	**0.039**
E_H:as.factor(Energy)44 ($k_{E_H}^{44}$)	−0.013 169	0.004 180	**0.002**
E_H:as.factor(Energy)46 ($k_{E_H}^{46}$)	−0.015 749	0.004 180	**<0.001**
Density (k_ρ)	0.395 350	0.182 103	**0.031**
Density:as.factor(Energy)42 (k_ρ^{42})	−0.265 340	0.257 533	0.304
Density:as.factor(Energy)44 (k_ρ^{44})	−0.237 566	0.257 533	0.357
Density:as.factor(Energy)46 (k_ρ^{46})	−0.090 163	0.257 533	0.727
Multiple R-squared:	0.9861		
Adjusted R-squared:	0.9856		
p-value:	**<0.001**		

($p<0.05$) at 42, 44, and 46 kVp in the absence of beam hardening but only at 46 kVp when the beam was hardened.

Based on these analyses, a new linear model [Eq. (6)] was fit for absorbance as a function of E_H alone with energy as a factor when the beam was hardened. The parameters obtained for this model are summarized in Table V. Once again, the slope of absorbance as a function of E_H was significant (k_{E_H}, $p<0.001$). The negative slopes for the energy-dependent effects of E_H were significant at 44 and 46 kVp ($k_{E_H}^{44}$ and $k_{E_H}^{46}$), and the absolute values were smaller than the slope for the energy-independent effect of E_H (k_{E_H}).

IV. DISCUSSION

We hypothesized and provide experimental evidence that x-ray absorbance can be modulated by the distance between covalently linked K-edge attenuating atoms like iodine. More specifically, x-ray absorbance by iodine is related to

TABLE IV. Parameters for a linear model of absorbance (A) as a function of harmonic error (E_H) and density (ρ) at different beam energies (E) with beam hardening. The model includes both energy-dependent and energy-independent relationships of absorbance to E_H and density. Linear model: $A=(I+I^E)+(k_{E_H}+k_{E_H}^E)\times E_H+(k_\rho+k_\rho^E)\times\rho$.

Coefficients	Estimate	Std. Error	p
INTERCEPT (I)	−0.143 473	0.282 349	0.612
as.factor(Energy)42 (I^{42})	−0.277 829	0.399 302	0.487
as.factor(Energy)44 (I^{44})	−0.125 670	0.399 302	0.753
as.factor(Energy)46 (I^{46})	−0.349 424	0.399 302	0.382
SLOPE			
E_H (k_{E_H})	0.021 908	0.004 122	**<0.001**
E_H:as.factor(Energy)42 ($k_{E_H}^{42}$)	−0.008 294	0.005 829	0.156
E_H:as.factor(Energy)44 ($k_{E_H}^{44}$)	−0.010 299	0.005 829	0.078
E_H:as.factor(Energy)46 ($k_{E_H}^{46}$)	−0.020 400	0.005 829	**0.001**
Density (k_ρ)	0.306 543	0.253 942	0.228
Density:as.factor(Energy)42 (k_ρ^{42})	0.237 206	0.359 128	0.509
Density:as.factor(Energy)44 (k_ρ^{44})	0.048 132	0.359 128	0.893
Density:as.factor(Energy)46 (k_ρ^{46})	0.212 491	0.359 128	0.555
Multiple R-squared:	0.9853		
Adjusted R-squared:	0.9848		
p-value:	**<0.001**		

TABLE V. Parameters for a linear model of absorbance (A) as a function of harmonic error (E_H) at different beam energies (E) with beam hardening. The model includes both energy-dependent and energy-independent relationships of absorbance to E_H. Linear model: $A=(I+I^E)+(k_{E_H}+k^E_{E_H})\times E_H$

Coefficients	Estimate	Std. Error	p
INTERCEPT (I)	0.197 353	0.002 019	<**0.001**
as.factor(Energy)42 (I^{42})	−0.014 094	0.002 856	<**0.001**
as.factor(Energy)44 (I^{44})	−0.072 155	0.002 856	<**0.001**
as.factor(Energy)46 (I^{46})	−0.113 168	0.002 856	<**0.001**
SLOPE			
E_H (k_{E_H})	0.025 164	0.003 160	<**0.001**
E_H:as.factor(Energy)42 ($k^{42}_{E_H}$)	−0.005 774	0.004 469	0.197
E_H:as.factor(Energy)44 ($k^{44}_{E_H}$)	−0.009 788	0.004 469	**0.029**
E_H:as.factor(Energy)46 ($k^{46}_{E_H}$)	−0.018 143	0.004 469	<**0.001**
Multiple R-squared:	0.9847		
Adjusted R-squared:	0.9844		
p-value:	<0.001		

the distance between iodine atoms, the x-ray photon energy, and iodine's K-shell energy. However, the mechanism of this relationship requires elucidation.

IV.A. Mixture rule

The mixture rule suggests that the mass attenuation coefficient of a material is the weighted sum of the mass attenuation coefficients of its constitutive elements. The observation that iodomethane+nonane absorbance was significantly greater than absorbance of iodomethane alone is consistent with the mixture rule. However, the mixture rule cannot explain the difference observed between iododecane and iodomethane+nonane. Both solutions have equal numbers of iodine and carbon atoms.

Furthermore, the observation that diiodomethane absorbance was significantly greater than 2× iodomethane absorbance is also inconsistent with the mixture rule, which would predict that 2× iodomethane absorbance should be equal to or greater than diiodomethane absorbance. Iodomethane (2×) has twice as many carbons and hydrogen atoms as diiodomethane. Additionally, the number of electrons per gram is significantly higher in the 2× iodomethane phantom than 1× diiodomethane.

The mixture rule also does not explain the apparent differences in x-ray absorbance between the structurally isomeric diiodobenzene molecules. For example, 1,3-diiodobenzene absorbance was significantly greater than 1,2-diiodobenze and 1,4-diiodobenzene absorbance. All three compounds have identical molecular formulae. Likewise, 2,6-diiodo-4-nitroaniline absorbance was not significantly different from 1,3-diiodobenzene absorbance despite the additional two nitrogen and two oxygen atoms. Importantly, carbon, nitrogen, and oxygen should not contribute significantly to x-ray absorbance due to x-ray photons produced by the 42 kVp tube voltage.

The findings in this study are consistent with previous studies which have demonstrated that the mixture rule can well approximate mass absorbance of biological samples, but it is not well suited for determining the mass attenuation coefficient of compounds.[9,10] Two explanations are that density or the interatomic distances play a role in x-ray absorbance.

IV.B. Density

Absorbance of iodomethane, iodomethane+nonane, and iododecane solutions are inconsistent with the observed absorbance differences attributable to density. Iodomethane+nonane absorbance is significantly higher than absorbance of iodomethane alone despite decreased iodomethane+nonane density (theoretical and experimental). One might argue that this effect is simply due to a greater number of carbon atoms provided by the nonane (electrons per gram), which increases scattering events in this energy range. This particular interpretation does not agree with the observation that iododecane, a molecule that has equal numbers of carbon and iodine atoms as the iodomethane+nonane solution, has a higher absorbance than iodomethane and iodomethane+nonane. Additionally, iododecane solution density was significantly lower than iodomethane. There was no significant difference in experimentally measured density between iododecane and iodomethane+nonane. These data suggest that large photoelectric attenuating atoms covalently linked to non-K-edge attenuating groups increase absorbance. Future research aimed at elucidating the mechanism of x-ray absorbance in these compounds may reveal how a carbon chain translates x-ray photon interaction to the K-shell of iodine via an apparent wave-function-like effect.

For the 2× iodomethane and diiodomethane experiments, on the other hand, the difference in absorbance could potentially be explained by differences in density between these two solutions, as shown in Table II. However, this interpretation is confounded by the inability to detect absorbance differences between the two samples at high tube voltages. At higher x-ray energies, the number of x-ray-dependent interaction should decrease as observed. However, the relative contribution of photon scattering events, dependent on mate-

rial density should conversely increase. Likewise, there was no significant absorbance difference between the samples at low tube voltages (40 kVp). The predominant difference between the two samples occurred when tube voltage was between 42 and 44 kVp. This suggests two things. First, these tube voltages (42–44 kVp) were high enough to produce significantly more photons with energies near the iodine K-shell energy (33.2 keV, see Table I) for photoelectric interaction with iodine atoms. Secondly, the difference in x-ray absorbance between the two samples suggests that the principal attenuating mechanism may be photoelectric in nature.

The absorbance measurements of diiodomethane, three positional isomers of diiodobenzene (1,2-diiodo benzene, 1,3-diiodo benzene, and 1,4-diiodo benzene) and 2,6-diiodo-4-nitroaniline are incongruous with the hypothesis that absorbance differences are dependent solely on density differences. Our data suggest that density is not a significant determinant of absorbance over the range of beam energies tested with beam hardening. In our experiments, the relationship between absorbance and density was only significant for an unfiltered beam. This suggests that the role of density is diminished when incident energy is concentrated near the iodine K-edge. Therefore, density cannot explain absorbance differences, with beam hardening, between compounds.

IV.C. Mass attenuation

The mass attenuation coefficients for all diiodinated molecules were obtained from the XCOM database in order to compare individual compound characteristics to absorbance. The weight fraction of solute was estimated using the experimentally determined density. The transmission factor [Eq. (2)] was calculated using the experimental density. A linear model relating measured absorbance to estimated transmission factor yielded results (data not shown) similar to the linear model of absorbance and density, as one would expect for the following reasons. First, the transmission factor is estimated using experimental densities, which were not significantly different between samples. The fact that the XCOM values are based on nonsignificantly different density values suggests that the mass attenuation coefficients should also not be significantly different. Second, the XCOM database does not distinguish between positional isomers.

The same calculation could not be performed with the theoretical densities because only two diiodinated compounds were liquids at room temperature (diiodomethane and 1,2-diiodobenzene). Therefore, additional studies with diiodinated molecules with known solution densities would be required to address this question.

IV.D. Harmonic error

Our data suggest that E_H is a strong determinant of absorbance over the range of beam energies tested. Further, the steepness of the relationship of absorbance to E_H declines as the beam energy moves away from the iodine K-edge, suggesting that E_H is likely related to a K-characteristic x-ray interaction. Also, this decline is significant at higher energies when the beam is hardened in comparison to when it is not. This further suggests that x-ray absorbance by the diiodo compounds tested is strongly related to E_H, particularly at energies close to the iodine K-edge.

It is assumed that the radius of the K-shell is relevant for the photoionization process. For iodine, the K-shell radius can be estimated by the Hartree approximation of $r_K = a_o/(Z-2)$, where a_o is the K-shell Bohr radius (0.5 Å), and Z is the atomic number of iodine (53). Hartree's approximation yields a K-shell radius for iodine of 0.98×10^{-2} Å, which is orders of magnitude smaller than the wavelength of a 33.2 keV x-ray photon ($\lambda_{K,I}=0.3758$ Å). This is a condition where one could assume a homogeneous wave field and thus a harmonic pseudo-oscillatory condition. The interiodine distance on a molecule such as diiodomethane is an order of magnitude greater (3.235 Å) than the iodine photoionizing wavelength ($\lambda_{K,I}$). Therefore, interiodine distance should have little to no effect on x-ray absorbance.

Shrimpton demonstrated that for many liquids, measured electron density quantified by Compton scattering techniques correlates well with the theoretical electron density.[11] Compounds containing large attenuating atoms such as chlorine fell off the line of identity. This discrepancy was attributed to calibration and systematic errors. However, Shrimpton's observation that highly attenuating atoms do not follow the predicted line of identity is consistent with the results of this study, which demonstrate that absorbance is enhanced when a photoelectric attenuating atom is covalently bonded to any other atom(s). This observation holds for both the finding that iododecane absorbance was greater than absorbance from a combination of iodomethane+nonane and that diiodomethane absorbance was significantly greater than the absorbance of twice the concentration of iodomethane.

IV.E. Mechanisms

It is well established that molecular bonding modulates x-ray absorbance as demonstrated by the many different X-ray absorption fine structure studies using x-ray spectroscopy.[12–14] However, these differences in absorbance represent relatively small perturbations relative to the K-edge absorbance threshold. It is unclear whether the integral of total absorbance over the entire region is sufficient to observe a 7% difference in total x-ray absorbance as observed between diiodomethane and 1,3-diiodobenzene for example. Further studies are needed to address this potential mechanism.

An alternative explanation is that the spacing between K-edge attenuating atoms modulates absorbance by a diffractive mechanism. Specifically, when atomic spacing is a wavelength harmonic of the incident photon, the integrated intensity of the diffraction pattern within the limits of the x-ray detector may fall to a local minimum.

The apparent photon interaction translating effect of molecules bound to K-edge attenuating atoms may occur via a similar mechanism to that demonstrated by Xie and colleagues.[15] In that study, they demonstrate that the material of a Young's double slit experiment can significantly impact photoelectric transmission through a double slit by a mecha-

nism of inductive electromagnetic fields created in the material. These data may suggest that on a molecular level, an incident photon may in fact interact with the entire molecule, setting up a field which may facilitate photon attenuation.

Lastly, the interaction could be consistent with the Copenhagen Interpretation of Young's double slit experiment, which suggests that a photon interacts with both slits but does not spatially resolve until it is measured. In this study, the openings, or slits, of Young's double slit experiment correspond to strong photoelectrically attenuating atoms on a molecule, and the obstacle in the double slit experiment is electromagnetically transparent matter. In effect, this manuscript describes a molecular double obstacle rather than the double slit experiment. Under this interpretation, the data might fit a hypothesis that the predominant mechanism underlying the relationship between absorbance and harmonic error is due to K-characteristic x-ray attenuation with iodine. Briefly, we demonstrate that absorbance and harmonic error are positively correlated when the effective beam energy (33.4 kV) is near the iodine k-edge energy (33.2 keV). The slope of the linear correlation (E_H) decreases as effective beam energy is increased, meaning that the strong relationship between absorbance and harmonic error decreases for higher energies. Therefore, if a K-characteristic x-ray photon arrives at the molecule and interacts with both iodine atoms, the photon may have a lower probability of resolving and interacting with either atom if those atoms are placed at a distance close to the harmonic error. Conversely, the probability of K-characteristic x-ray interaction with either iodine atom could increase if the atoms are placed at distances with a harmonic error greater than 0.

Regardless of the mechanism by which absorbance increases in these compounds, this study raises the intriguing possibility that an entirely new class of conformationally active compounds for modulating x-ray absorbance can be created for the purpose of measuring biophysical parameters such as, but certainly not limited to, membrane potential, chemical concentrations, or even possibly resolving noncrystallized protein structures using x-ray attenuating atoms instead of large fluorophores as used in Förster resonance energy transfer.[16] This can be done by making molecules that vary the distance between strong K-edge attenuating atoms in response to external stimuli.

IV.F. Limitations

This study utilized a polychromatic x-ray beam from a fluoroscope instead of monochromatic photons capable of further elucidating the direct mechanism by which absorbance occurs. Future studies with monochromatic x-ray sources may shed light on the precise mechanisms underlying the observed phenomenon.

It is important to note that the relationship between absorbance and harmonic error is significant for a relatively small number of compounds presented herein. Additional studies aimed at elucidating the mechanism of the observed absorbance dependence on x-ray K-edge attenuating atomic distances may strengthen the use of harmonic error as the mathematical relationship, or may elucidate a stronger mathematical relationship between absorbance and K-edge attenuating atomic distances.

While the mass thickness is an important descriptor of density effects on absorbance, measurements in this study controlled for the path length and not mass thickness. This, however, was done to minimize experimental errors associated with density measurements. We could not measure statistical differences in density, and as a result, would be unable to control for mass thickness. In order to account for resulting density effects, density was included in the linear model for absorbance.

Importantly, these limitations do not detract from the principal finding, which suggests that x-ray absorbance in molecules with multiple K-edge attenuating atoms is greatest when the distance between those atoms is greater than a harmonic of the associated K-characteristic photon wavelength.

ACKNOWLEDGMENTS

We thank Peter Jenkins for his generous assistance with calibrating the fluoroscope. This study was supported by a grant from the Nora Eccles Treadwell Foundation awarded to Dr. Poelzing.

[a]Author to whom correspondence should be addressed. Tel: (801) 585-1862. FAX: (801) 581-3128. Electronic mail: poelzing@cvrti.utah.edu

[1]W. B. Cannon and A. Moser, "The movements of the food in the esophagus," Am. J. Physiol. **1**, 435–444 (1898).
[2]T. M. Harned and L. Mascarenhas, "Severe methotrexate toxicity precipitated by intravenous radiographic contrast," J. Pediatr. Hematol. Oncol. **29**(7), 496–499 (2007).
[3]M. G. Stabin, T. E. Peterson, G. E. Holburn, and M. A. Emmons, "Voxel-based mouse and rat models for internal dose calculations," J. Nucl. Med. **47**(4), 655–659 (2006).
[4]M. Vermess, D. C. Chatterji, J. L. Doppman, G. Grimes, and R. H. Adamson, "Development and experimental evaluation of a contrast medium for computed tomographic examination of the liver and spleen," J. Comput. Assist. Tomogr. **3**(1), 25–31 (1979).
[5]F. Stacul, "Current iodinated contrast media," Eur. Radiol. **11**(4), 690–697 (2001).
[6]A. W. Leber, A. Knez, A. Becker, C. Becker, M. Reiser, G. Steinbeck, and P. Boekstegers, "Visualising noncalcified coronary plaques by CT," Int. J. Card. Imaging **21**(1), 55–61 (2005).
[7]T. S. Curry, J. E. Dowdey, and R. C. Murry, Jr. *Christensen's Physics of Diagnostic Radiology.* 4th Ed. (Lippincott Williams & Wilkins, New York, 1990).
[8]B. R. Brooks, R. E. Bruccoleri, B. D. Olafson, D. J. States, S. Swaminathan, and M. Karplus, "CHARMM: A program for macromolecular energy, minimization, and dynamics calculations," J. Comput. Chem. **4**(2), 187–217 (1983).
[9]U. Turgut, E. Buyukkasap, O. Simsek, and M. Ertugrul, "X-ray attenuation coefficients of Fe compounds in the K-edge region at different energies and the validity of the mixture rule," J. Quant. Spectrosc. Radiat. Transf. **92**(2), 143–151 (2005).
[10]U. Turgut, O. Simsek, E. Buyukkasap, and M. Ertugrul, "X-Ray attenuation coefficients at different energies and the validity of the mixture rule for compounds around the absorption edge," Spectrochim. Acta, Part B **57**(2), 261–266 (2002).
[11]P. C. Shrimpton, "Electron density values of various human tissues: in vitro Compton scatter measurements and calculated ranges," Phys. Med. Biol. **26**(5), 907–911 (1981).
[12]H. Sakane, T. Mitsui, H. Tanida, and I. Watanabe, "XAFS analysis of triiodide ion in solutions," J. Synchrotron Radiat. **8**(Pt. 2), 674–676 (2001).
[13]M. Harada, H. Satou, and T. Okada, "Hydration structures of bromides on cationic micelles," J. Phys. Chem. B **111**(42), 12136–12140 (2007).

[14]P. Lindqvist-Reis, I. Persson, and M. Sandstrom, "The hydration of the scandium(III) ion in aqueous solution and crystalline hydrates studied by XAFS spectroscopy, large-angle X-ray scattering and crystallography," Dalton Trans. **28**(32), 3868–3878 (2006).
[15]M. Mansuripur, Yong Xie, A. R. Zakharian, and J. V. Moloney, "Transmission of light through slit apertures in metallic films," IEEE Trans. Magn. **41**(2), 1012–1015 (2005).
[16]E. Kobrinsky, E. Schwartz, D. R. Abernethy, and N. M. Soldatov, "Voltage-gated mobility of the Ca2+ channel cytoplasmic tails and its regulatory role," J. Biol. Chem. **278**(7), 5021–5028 (2003).